

---

# A LOW-COST NEURAL ODE WITH DEPTHWISE SEPARABLE CONVOLUTION FOR EDGE DOMAIN ADAPTATION ON FPGAs

---

A PREPRINT

**Hiroki Kawakami**

Keio University  
3-14-1 Hiyoshi, Kohoku-ku, Yokohama, Japan  
kawakami@arc.ics.keio.ac.jp

**Hirohisa Watanabe**

Keio University  
3-14-1 Hiyoshi, Kohoku-ku, Yokohama, Japan  
watanabe@arc.ics.keio.ac.jp

**Keisuke Sugiura**

Keio University  
3-14-1 Hiyoshi, Kohoku-ku, Yokohama, Japan  
sugiura@arc.ics.keio.ac.jp

**Hiroki Matsutani**

Keio University  
3-14-1 Hiyoshi, Kohoku-ku, Yokohama, Japan  
matutani@arc.ics.keio.ac.jp

July 28, 2021

## ABSTRACT

Although high-performance deep neural networks are in high demand in edge environments, computation resources are strictly limited in edge devices, and light-weight neural network techniques, such as Depthwise Separable Convolution (DSC), have been developed. ResNet is one of conventional deep neural network models that stack a lot of layers and parameters for a higher accuracy. To reduce the parameter size of ResNet, by utilizing a similarity to ODE (Ordinary Differential Equation), Neural ODE repeatedly uses most of weight parameters instead of having a lot of different parameters. Thus, Neural ODE becomes significantly small compared to that of ResNet so that it can be implemented in resource-limited edge devices. In this paper, a combination of Neural ODE and DSC, called dsODENet, is designed and implemented for FPGAs (Field-Programmable Gate Arrays). dsODENet is then applied to edge domain adaptation as a practical use case and evaluated with image classification datasets. It is implemented on Xilinx ZCU104 board and evaluated in terms of domain adaptation accuracy, training speed, FPGA resource utilization, and speedup rate compared to a software execution. The results demonstrate that dsODENet is comparable to or slightly better than our baseline Neural ODE implementation in terms of domain adaptation accuracy, while the total parameter size without pre- and post-processing layers is reduced by 54.2% to 79.8%. The FPGA implementation accelerates the prediction tasks by 27.9 times faster than a software implementation.

**Keywords** Neural ODE · Depthwise separable convolution · Domain adaptation · Distillation · FPGA

## 1 Introduction

Deep neural networks especially CNNs (Convolutional Neural Networks) for image recognition tasks stack more layers and parameters in order to gain a higher accuracy. Although such image recognition tasks are in high demand in edge environments, computation resources are strictly limited in edge devices, decreasing the possibility to utilize high-performance deep neural network models. To address this issue, light-weight neural network models have been developed [1][2]. Their key idea to reduce the number of parameters is DSC (Depthwise Separable Convolution) that decomposes a conventional convolutional layer into two smaller convolutional steps. Assuming  $K$  is a convolutional kernel size of one side, the order of the parameter size is reduced to  $\approx 1/K^2$ .

ResNet [3] is one of conventional deep neural network models that stack a lot of layers and parameters for a higher accuracy because it can address the vanishing gradient problem by introducing shortcut connections. To reduce the

parameter size of ResNet, by utilizing a similarity to ODE (Ordinary Differential Equation), Neural ODE [4] repeatedly uses most of weight parameters instead of having a lot of different parameters. More specifically, ResNet consists of sets of layers or building blocks. An input to a building block is added to an output of the block via a shortcut connection for the residual learning. This stacking structure of ResNet is interpreted as an ODE solver, and one execution of a building block is interpreted as one step of the ODE solver. By repeatedly executing the same building block  $C$  times instead of implementing  $C$  different building blocks, the parameter size of these  $C$  blocks in ResNet is theoretically reduced to  $\approx 1/C$ . Thus, Neural ODE becomes significantly small compared to that of ResNet, can be implemented in resource-limited edge devices. Recently its implementation on a low-end FPGA (Field-Programmable Gate Array) device has been reported in [5]. However, its performance improvement is limited since only one or two building blocks are implemented on the programmable logic, while it does not employ any other parameter reduction techniques, such as DSC.

In this paper, a combination of Neural ODE and DSC, called dsODENet, is designed and implemented for FPGAs. As a practical use case, dsODENet is applied to edge domain adaptation, in which knowledge obtained at source domain is adapted to a different domain called target domain. It is useful in a common edge AI deployment scenario, in which trained parameters at cloud side are deployed to edge devices by addressing data distribution difference or domain shift between the trained environment and deployed edge environment. dsODENet is implemented on Xilinx ZCU104 board by Xilinx Vivado HLS and evaluated in terms of the domain adaptation accuracy using image classification datasets, training speed, FPGA resource utilization, and speedup rate compared to a software execution.

The rest of this paper is organized as follows. Section 2 introduces baseline technologies behind our proposal, such as DSC, Neural ODE, and domain adaptation. Section 3 proposes dsODENet for FPGA-based domain adaptation. Section 4 evaluates it in terms of accuracy, training speed, FPGA resource utilization, and execution time. Section 5 concludes this paper.

## 2 Related Work

### 2.1 Depthwise Separable Convolution

CNNs typically have a lot of convolutional layers for a higher image recognition accuracy. The parameter size of a convolutional layer can be calculated as a product of the number of input channels, the number of output channels, and kernel size. DSC [1][2] is a technique to significantly reduce the parameter size of convolutional layers. It decomposes a conventional convolutional layer into two smaller convolutional steps: Depthwise Convolution step and Pointwise Convolution step. They are illustrated in Figures 1 and 2.

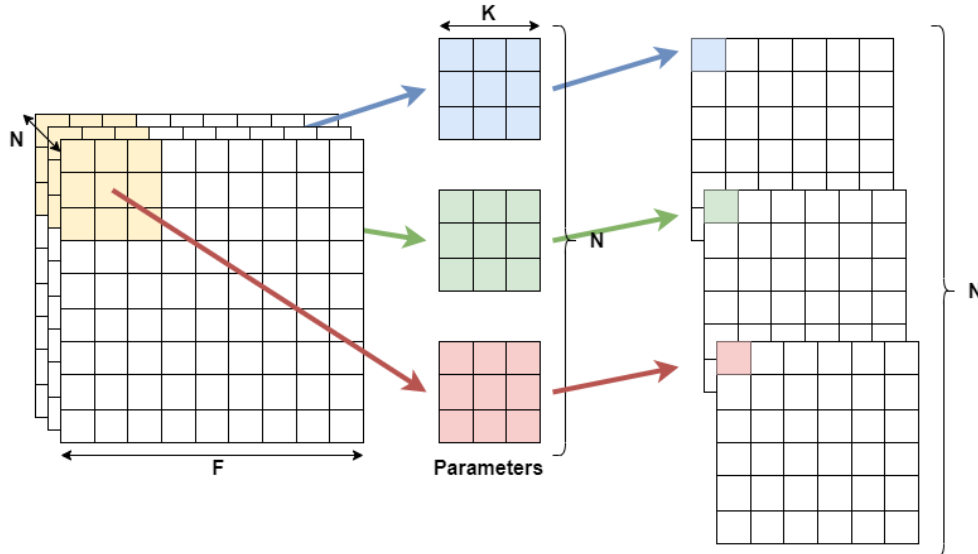


Figure 1: Depthwise Convolution step

Let  $F$ ,  $N$ ,  $M$ , and  $K$  be the feature map size of one side, the number of input channels, the number of output channels, and the kernel size of one side, respectively. In the conventional convolutional layer, a convolutional operation involv-

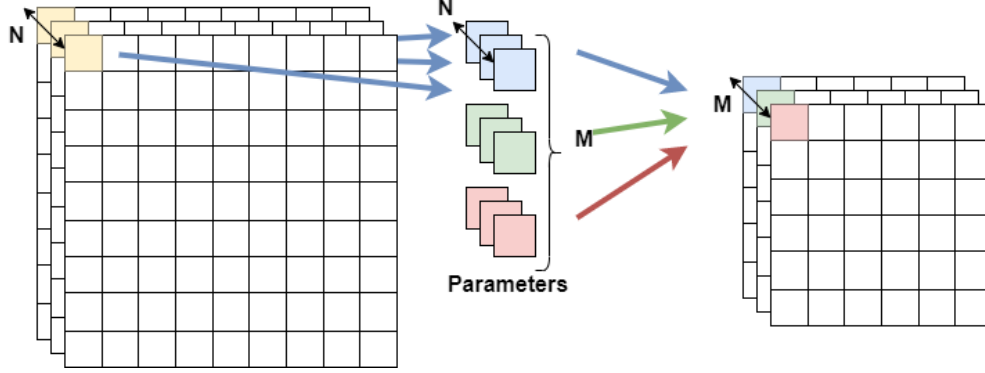


Figure 2: Pointwise Convolution step

ing both spatial and channel directions (the size is  $NK^2$ ) is applied for each of input feature map. Different weight parameters are used for each of  $M$  output channels; thus the weight parameter size is  $NMK^2$  in total.

In DSC, as Depthwise Convolution step, as shown in Figure 1, a convolutional operation involving spatial direction only (the size is  $K^2$ ) is applied for each of input feature map. Different weight parameters are used for each of  $N$  input channels; thus its weight parameter size is  $NK^2$ . Then, an output feature map of the Depthwise Convolution step (Figure 1 right) is fed to the Pointwise Convolution step as an input feature map. As shown in Figure 2, a  $1 \times 1$  convolutional operation is applied for each of the input feature map and for each of  $M$  output channels. The weight parameter size is thus  $NK^2 + NM$  in total.

When  $N = 128$ ,  $M = 256$ , and  $K = 3$ , the parameter size of a conventional convolutional layer is 294,912. In the case of DSC, the parameter size of a convolutional layer is  $1,152 + 32,768 = 33,920$ . Assuming that  $K = 3$  and the numbers of channels ( $N$  and  $M$ ) are greater than  $K$ , the parameter size is reduced to approximately 1/8 to 1/9. In this example, DSC reduces the parameter size of a convolutional layer to 11.5%.

## 2.2 Ordinary Differential Equation

ODE is an ordinary differential equation that contains an unknown function and its derivatives. An example of a first-order differential equation is shown in Equation 1.

$$\frac{dz}{dt} = f(z(t), t, \theta), \quad (1)$$

where  $f(\cdot)$  is a known function and  $\theta$  is the parameter. When the initial value  $z(t_0)$  is given, a problem to find  $z(t_1)$  that satisfies Equation 1 is known as an initial value problem. The solution is formulated as shown in Equation 2.

$$z(t_1) = z(t_0) + \int_{t_0}^{t_1} f(z(t), t, \theta) dt \quad (2)$$

In the right side of Equation 2, the second term contains an integral of the function, and thus it cannot be solved analytically for arbitrary functions. To solve the solution approximately, the following ODEsolve function is introduced.

$$z(t_1) = \text{ODESolve}(z(t_0), t_0, t_1, f) \quad (3)$$

As an ODEsolve function, Euler method shown in Equation 4 can be used.

$$z(t_{i+1}) = z(t_i) + hf(z(t_i), t_i, \theta) \quad (4)$$

Euler method is a first-order approximation for solving the initial value problem, and it is used in this paper.

## 2.3 Neural ODE

ResNet is a well-known neural network architecture that can increase the number of stacked layers or building blocks by introducing shortcut connections. Using a shortcut connection, an input feature map to a building block is temporarily saved and then it is additionally added to the original output of the building block to generate the final output of the block. Let  $z_t$ ,  $\theta$ , and  $f(z_t, \theta_t)$  be an input feature map to a building block, parameters of the building block, and processing result of the block, respectively. The final output of the building block is represented as Equation 5.

$$z_{t+1} = f(z_t, \theta_t) + z_t \quad (5)$$

Please note that Equation 5 is similar to Equation 4, though the former basically assumes vector values while the latter assumes scalar values. Based on this similarity, one building block is interpreted as one step of Euler method. Euler method is a first-order method. Assuming that ODESolve is replaced with Euler method, it can be interpreted that a first-order approximation is applied to solve the output of the building block. In this paper, one building block is called ODEBlock and the whole network architecture consisting of ODEBlocks is called ODENet.

Figure 3 illustrates a practical example of ODENet. The left side of Figure 3 shows the overall ODENet architecture

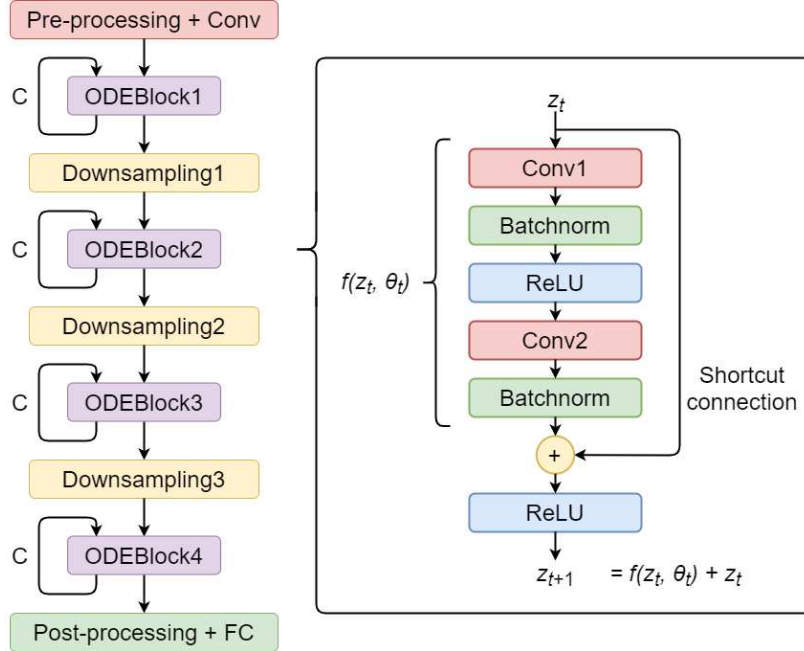


Figure 3: ODENet architecture

that consists of ODEBlocks and downsampling blocks in addition to pre-processing and post-processing layers. The pre-processing layer has a convolutional layer (denoted as Conv1) and the post-processing layer has a fully-connected layer (denoted as FC). The right side of Figure 3 shows the internal structure of an ODEBlock that consists of convolutional layers, batch normalization layers (denoted as Batchnorm), and ReLU layer. Please note that each ODEBlock is repeatedly executed  $C$  times in this example. In ResNet,  $C$  different building blocks are executed once while in ODENet, the same ODEBlock is repeatedly executed  $C$  times. Let  $O(L)$  be the parameter size of one building block or ODEBlock. Total parameter sizes of ResNet and ODENet are  $O(CL)$  and  $O(L)$ , respectively; thus ODENet can significantly reduce the parameter size.

## 2.4 Edge Domain Adaptation

Domain adaptation is a kind of transfer learning, where knowledge obtained at a source domain is transferred to a different domain called target domain. It is typically assumed that the source domain has enough labeled training data while the target domain does not. It is useful in a common edge AI deployment scenario, in which trained parameters at cloud side are deployed to edge devices by addressing data distribution difference or domain shift between the trained environment and deployed edge environment. MobileDA [6] is a domain adaptation technique for edge devices based on knowledge distillation technique. Since the target domain is an edge environment in the edge domain adaptation scenario, the target model should be further reduced in parameter size and computation cost. Although pruning, quantization, and distillation are very common model compression techniques, in this paper we propose a combination of ODENet (see Figure 3) and DSC (Depthwise Separable Convolution) to further reduce the parameter size of the target domain model.

In this paper, a modified version of MobileDA is used as an edge domain adaptation procedure to gain a higher performance. In our approach, one teacher model and two student models are used in the domain adaptation. ResNet is used as the teacher model, while the combination of ODENet and DSC, called dsODENet, is used in the two student models. In Section 4, our approach will be compared to the original MobileDA.

In our approach, the training phase consists of three steps. First, a teacher model is trained with source domain data in Step 1, and then two student models are trained in Steps 2 and 3. Since Step 1 is trivial, Steps 2 and 3 are illustrated in Figure 4. In Step 2, the teacher model is fixed (i.e., no update is allowed), and parameters of student model 1 are

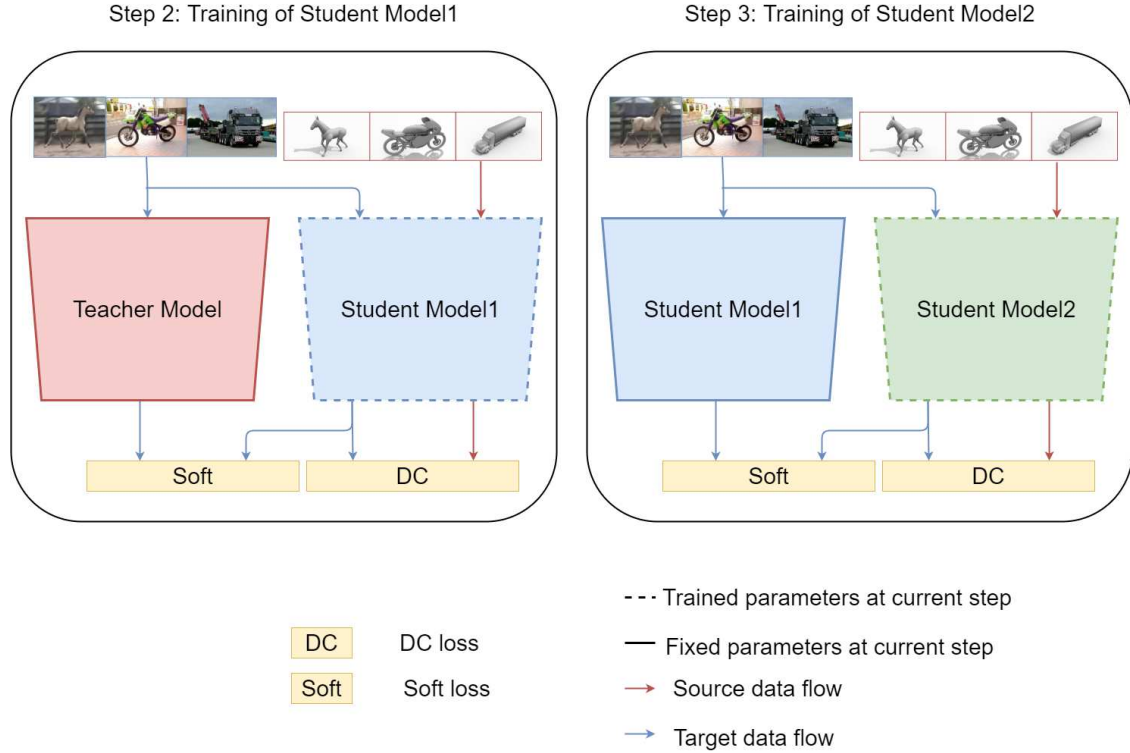


Figure 4: Training steps for two student models

trained by the help of the teacher model. In Step 3, the student model 1 is fixed, and parameters of student model 2 are trained by the help of the student model 1. Step 3 is optional, and thus either student model 1 or model 2 can be used for the prediction.

As shown in Figure 4, two loss functions are used in this domain adaptation:  $L_{Soft}$  and  $L_{DC}$ .  $L_{Soft}$  is a soft target loss of knowledge distillation and it is defined in Equation 6.  $L_{DC}$  is a loss function borrowed from Deep Coral [7] and it is defined in Equation 7.

$$L_{Soft} = \mathbb{E}_{(x_t) \sim (X_t)} \sum_k [L(M_T(x_t), M_S(x_t))] \quad (6)$$

$$L_{DC} = \frac{1}{4d^2} \|C_s - C_t\|_F^2, \quad (7)$$

where  $L(\cdot)$  is a loss function,  $M_S(x_t)$  is an output when target domain data is fed to a student model,  $M_T(x_t)$  is an output when target domain data is fed to a teacher model,  $C_s$  is a covariance matrix of  $M_S(x_s)$ ,  $C_t$  is a covariance matrix of  $M_S(x_t)$ ,  $d$  is degree of the covariance matrix (e.g., the number of samples), and  $\|\cdot\|_F^2$  is Frobenius norm, respectively. Given that target domain labels are produced by a teacher model,  $L_{Soft}$  is a loss value computed by comparing the generated target domain labels and those predicted by a student model.  $L_{DC}$  is computed by the distance between the covariance matrixes of the two domains. The final loss function combines  $L_{Soft}$  and  $L_{DC}$  as shown in Equation 8.

$$L = L_{Soft} + \lambda L_{DC} \quad (8)$$

$L_{DC}$  is weighted by a hyper-parameter  $\lambda$  that controls the strength of domain confusion. That is, a smaller  $\lambda$  increases the importance of class prediction results by a teacher model, which was trained by the source domain data. On the other hand, a larger  $\lambda$  increases the importance of domain invariant representation, but class prediction accuracy may be weakened.

Please note that target domain samples to be trained are selected by a given threshold value. More specifically, target domain samples are first fed to the teacher model. Softmax function is then applied to the class prediction results so that the sum of the probability of each class is 1.0. If the highest class probability value of a sample is greater than a given threshold value, the sample is used for the student model training. In other words, this can prevent situations that incorrect labels produced by the teacher model are used for the student model training.

### 3 Depthwise Separable Neural ODE for FPGA

#### 3.1 Models

To reduce parameter size, in this paper we propose to combine ODENet and DSC, called dsODENet, for edge devices, such as FPGAs. Figures 5 and 6 show two dsODENet models: model with two ODEBlocks and that with three ODEBlocks. They consist of two or three ODEBlocks and one or two downsampling blocks, respectively.

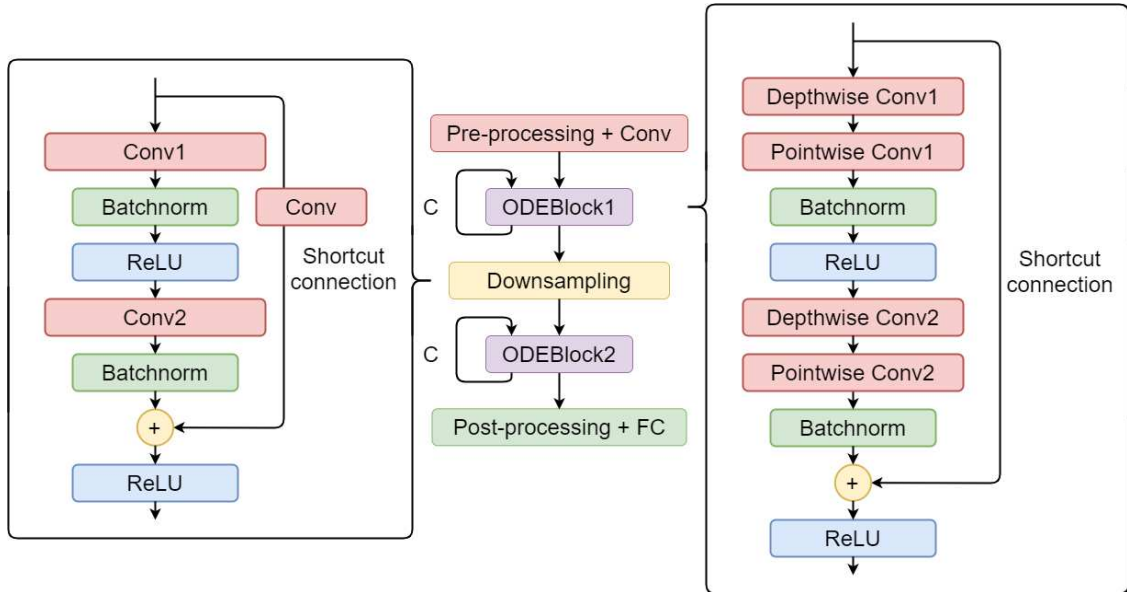


Figure 5: Model with two ODEBlocks

In Figure 5, the right box shows the internal structure of ODEBlock1 and the left box shows that of downsampling block. The structures of ODEBlocks and downsampling block are similar, but in the ODEBlocks, input and output feature map sizes are the same and  $M = N$ , while in downsampling block, input feature map size is scaled down to  $1/2 \times 1/2$  and  $M = 2N$ . Each ODEBlock is executed  $C$  times, while the downsampling block is executed once. In the downsampling blocks, a  $1 \times 1$  convolutional operation with padding size 2 is additionally applied to the shortcut connection. To reduce the parameter size of the two ODEBlocks case, DSC can be applied to convolutional layers of ODEBlocks and downsampling block. We observed that DSC on the downsampling block that rescales the feature map is sometimes sensitive to accuracy. Considering the stability, in the two ODEBlocks case, DSC is applied to the two ODEBlocks while it is not applied to the downsampling block, as shown in Figure 5. Assuming that  $N$  is 64 in ODEBlock1, parameter sizes of ODEBlock1, downsampling1, and ODEBlock2 in the ODENet without DSC are 73,728 + 229,376 + 294,912; thus the total size is 598,016. In dsODENet, their sizes are 9,344 + 229,376 + 35,072; thus the total size is 273,792, which is 54.2% reduction. Assuming a 32-bit fixed-point representation, their sizes are 19.1Mb and 8.8Mb.

As shown in Figure 6, the three ODEBlocks case has three ODEBlocks and two downsampling blocks. DSC is applied to all the three ODEBlocks. Regarding the downsampling blocks, their parameter sizes without DSC are 221,184 and 884,736, respectively, assuming that  $N$  is 64 in ODEBlock1. Their sizes depend on the numbers of input and output channels, and these numbers are doubled once the downsampling is applied; thus, the second downsampling block (Downsampling2) is much larger than that of the first one (Downsampling1). Since DSC on the downsampling block is sometimes sensitive to accuracy as mentioned above, in this paper DSC is applied only to the second downsampling block. Please note that parameter sizes of ODEBlock1, downsampling1, ODEBlock2, downsampling2, and ODE-

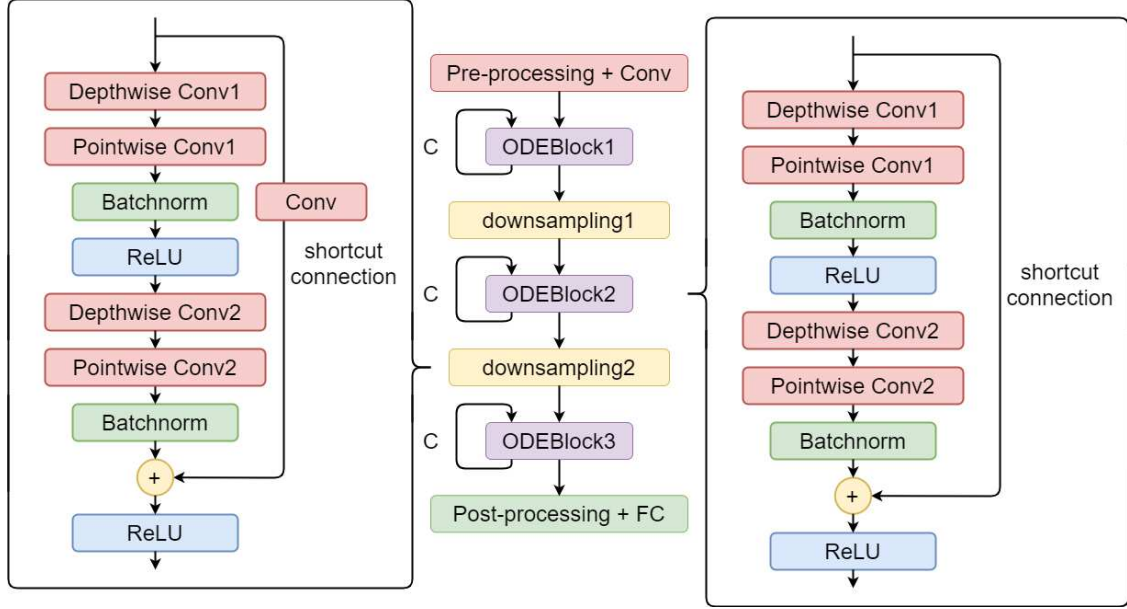


Figure 6: Model with three ODEBlocks

Block3 in the ODENet without DSC are  $73,728 + 229,376 + 294,912 + 917,504 + 1,179,648$ ; thus the total size is 2,695,168. In dsODENet, their sizes are  $9,344 + 229,376 + 35,072 + 134,528 + 135,680$ ; thus the total size is 544,000, which is 79.8% reduction. Assuming a 32-bit fixed-point representation, their sizes are 86.2Mb and 17.4Mb.

These parameter size reduction by DSC is significant since these parameters are implemented on BRAM or URAM of modest FPGA devices for simplicity in this paper. The following subsection illustrates an FPGA implementation of dsODENet. In the evaluations of Section 4, ResNet, ODENet, and dsODENet are used as student models of a domain adaptation mentioned in Section 2.4.

### 3.2 FPGA Implementation

As an implementation target, we assume SoC-type FPGA devices that consist of PL (programmable logic) and PS (processing system) parts, and we select Xilinx ZCU104 evaluation board in this paper. The proposed dsODENet models are designed with C/C++ language, and Xilinx Vivado HLS 2020.2 is used as a high-level synthesis tool. They are evaluated in terms of FPGA resource utilization and performance in Section 4.2.4. The operating frequency of PL part of the FPGA is set to 100MHz. A 32-bit fixed-point format is used to represent numbers.

The weight parameters and feature maps are implemented on BRAM or URAM of the FPGA to fully enjoy benefits of using fast on-chip memories. BRAM and URAM sizes are 11Mb and 27Mb in total, respectively. Their instance sizes are 36kb and 288kb. Please note that, depending on the number and sizes of parameter arrays, a part of BRAM and URAM instances is underutilized. In our design, each parameter array is carefully implemented on either BRAM or URAM instances to minimize the underutilized on-chip memories. In the case of the three ODEBlocks case, for example, parameter arrays of normal convolutional layers of Downsampling1, those of depthwise and pointwise convolutional layers of Downsampling2, and those of pointwise convolutional layers of ODEBlock3 are implemented in the URAM instances; and the others are implemented on BRAM instances. Regarding the feature maps, an input feature map array, an output feature map array, and a temporary feature map array that stores the input to be fed to the output directly via a shortcut connection are needed. Their sizes are varied depending on input image size, which is also varied by the Downsampling blocks. In our design, three image sizes evaluated in Section 4 are supported, and all of them are implemented on BRAM instances of the FPGA for a better flexibility.

## 4 Evaluations

In this section, the proposed dsODENet for FPGAs is evaluated with an edge domain adaptation scenario with image recognition datasets. For accuracy evaluations, it is implemented with Pytorch 1.8.1 and torchvision 0.9.1. For

resource utilization and performance evaluations, it is implemented with Xilinx Vivado v2020.2 for ZCU104 FPGA board. Specification of the ZCU104 board is shown in Table 1.

Table 1: Specification of ZCU104 board

OS	Pynq Linux (Ubuntu 18.04)
CPU	ARM Cortex-A53 @ 1.5GHz
DRAM	DDR4 2GB
FPGA	Zynq UltraScale+ XCZU7EV-2FFVC1156

## 4.1 Datasets

For accuracy evaluations, Office-31 dataset (Office-31 [8]), road signs datasets (Synth signs [9] and GTSRB [10]), and digit datasets (SVHN [11] and MNIST [12]) are used as the datasets. Their input image sizes are  $256 \times 256$ ,  $40 \times 40$ , and  $32 \times 32$ , respectively. The numbers of their classes are 31, 43, and 10. The amounts of their domain shifts are various, small, and large. The MNIST images are grayscale, while SVHN images are RGB colored; thus the MNIST images are duplicated for three channels so that they are compatible with the 3-channel SVHN images. Office-31 is a popular dataset used for domain adaption tasks. It contains 4,110 images, and they are divided into three domains: Amazon (A-domain), Webcam (W-domain), and DSLR (D-domain). The numbers of their images are 2817, 795, and 498, respectively. A $\rightarrow$ W means a domain adaptation scenario in which A-domain is a source domain and W-domain is a target domain. The numbers of W-domain and D-domain images are smaller than that of A-domain. A $\rightarrow$ W and A $\rightarrow$ D are examined in this paper because domain adaptation from a domain with more images to that with less images is a typical use case. The edge domain adaptation procedure proposed in Section 2.4 is used. All the labeled source domain data and all the unlabeled target domain data are used for the training phase. The accuracy is then evaluated with all the labeled target data.

## 4.2 Accuracy

SGD is used as an optimizer. The momentum is 0.9 and weight decay is 0. The learning rate is reduced based on Equation 9.

$$\eta = \frac{\eta_0}{(1 + \alpha p)^\beta}, \quad (9)$$

where  $\eta_0 = 0.01$ ,  $\alpha = 10$ ,  $\beta = 0.75$ , and  $p$  is linearly changed from 0 to 1. In the evaluations, the same experiments are executed three times and their accuracy values are averaged and reported. As a teacher model, an initial model is pre-trained with ImageNet dataset. Based on this initial model except for the final fully-connected layer, a teacher model is trained. Since all the layers except for the final layer are pre-trained, the learning rate is set to 1/10. Different student models that use ResNet-50, ODENet, and dsODENet are compared in terms of accuracy. ODENet and dsODENet use three ODEBlocks as shown in Figure 6. The number of executions  $C$  of an ODEBlock is set to 10. They are also compared to a teacher model of ResNet-50 and other domain adaptation techniques.

### 4.2.1 Office-31 Dataset

As a counterpart, MobileDA uses AlexNet as a student model and ResNet-50 as a teacher model. 80% of target domain data is used for the training. As another counterpart, CDAN [13] which is a domain adaptation based on adversarial training is also considered. Table 2 shows the evaluation results of CDAN, MobileDA, and our approach with different student models.

Table 2: Domain adaptation accuracy of Office-31 dataset

Model	A $\rightarrow$ W	A $\rightarrow$ D
CDAN [13]	77.9	75.1
MobileDA [6]	71.5	75.3
Teacher model ResNet-50	75.8	78.3
Student model ResNet-50	80.6	80.9
Student model ODENet	71.3	78.8
Student model dsODENet	72.7	79.1

“Student model dsODENet” is our domain adaptation method that uses dsODENet as a student model. Although it does not outperform its teacher model in terms of accuracy, it is better than the original MobileDA by 1.2% and 3.8% for A→W and A→D scenarios.

Figure 7 shows the training speeds of different student models (ResNet-50, ODENet, and dsODENet) for A→D scenario. As shown in the figure, the student model of ResNet-50 is converged faster than the others, followed by

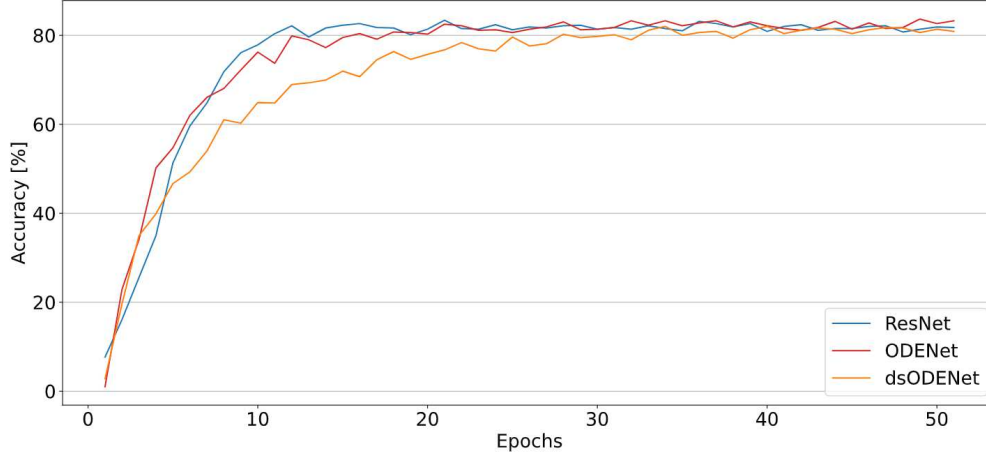


Figure 7: Training speed of different student models in Office-31 dataset

those of dsODENet and ODENet. As mentioned, a feature map size is 1/4 while the number of channels is doubled once a downsampling is applied. In ResNet-50, the number of implemented building blocks can be optimized for each feature map size. Actually these numbers are optimized in this experiment. These numbers in ResNet-50 are interpreted as the numbers of continuous executions of ODEBlocks in the cases of ODENet and dsODENet ( $C$  in Figures 5 and 6). As mentioned, in ODENet and dsODENet, a single execution of an ODEBlock is interpreted as a single step of Euler method. Reducing the number of executions  $C$  of an ODEBlock degrades the approximation performance and reduces the accuracy. As a result, to obtain a stable accuracy, the number of continuous executions  $C$  of an ODEBlock is equally set to 10 for each feature map size in ODENet and dsODENet cases. Since there is still a room for optimization, it slightly decreases the training speed due to unoptimized or unwanted executions depending on input image sizes. Please note that the training speed of dsODENet is faster than ODENet, because in dsODENet the number of parameters to be trained is reduced by 54.2% to 79.8% by DSC.

#### 4.2.2 Road Sign Dataset

As a counterpart, DSN [14] which is a domain adaptation based on adversarial training is compared to our approach with different student models. Table 3 shows the evaluation results of DSN and our approach with different student models. Please note that network structures of DSN and ours are different and a fair comparison is difficult. “Student

Table 3: Domain adaptation accuracy of road sign datasets

Model	Synth signs→GTSRB
DSN [14]	93.1
Teacher model ResNet-50	95.1
Student model ResNet-50	97.1
Student model ODENet	97.0
Student model dsODENet	97.1

model dsODENet” is our proposal, and its accuracy is higher than that of the teacher model by 2.0%. It is same as the student model of ResNet-50 and better than DSN. As shown, the accuracies of student models become higher than that of the teacher model because the two datasets contain a large enough number of images and their domain shift is small. As the domain shift is small, the accuracies of ResNet-50, ODENet, and dsODENet are similar.

### 4.2.3 Digit Dataset

As a counterpart, ADDA [15] which is also a domain adaptation based on adversarial training is considered. Table 4 shows the evaluation results of ADDA and our approach with different student models. “Student model dsODENet”

Table 4: Domain adaptation accuracy of digit datasets

Model	SVHN→MNIST
ADDA [15]	76.0
Teacher model ResNet-50	75.0
Student model ResNet-50	82.6
Student model ODENet	79.0
Student model dsODENet	80.7

is our proposal, and it is higher than the teacher model by 5.7%. It is better than ADDA. Figure 8 shows the training speeds of different student models (ResNet-50 and dsODENet) for SVHN→MNIST scenario. In Figure 8, six lines

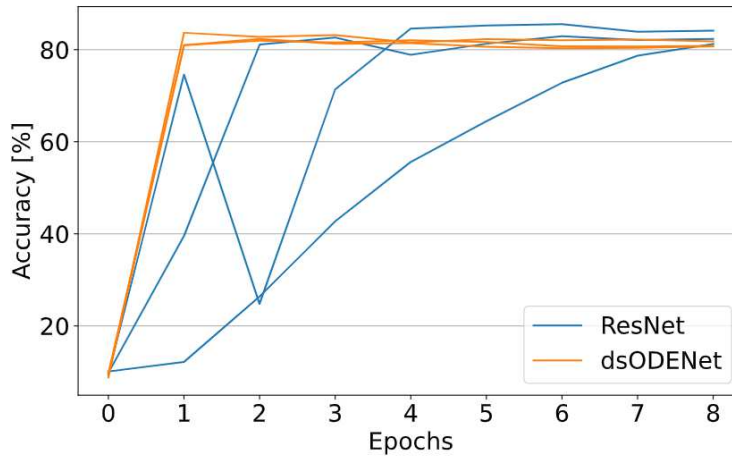


Figure 8: Training speed of different student models in digit datasets

are shown in total since ResNet-50 and dsODENet are trained three times each. dsODENet is converged fast and stable compared to ResNet-50 because the number of parameters of dsODENet is significantly reduced compared to ResNet-50. For domain adaptation tasks with a larger domain shift, the accuracy of ResNet-50 becomes higher than that of dsODENet but the training curve of dsODENet is still stable.

### 4.2.4 FPGA Resource and Performance

dsODENet is implemented on the FPGA and evaluated in terms of resource utilization and execution time. More specifically, dsODENets with two and three ODEBlocks are implemented on PL part of the FPGA, while only the pre- and post-processing layers are executed on PS part as a software. Table 5 shows resource utilizations when two ODEBlocks (Block2) and three ODEBlocks (Block3) are implemented. Please note that the weight parameter and

Table 5: FPGA resource utilization of dsODENet

	BRAM	DSP	FF	LUT	URAM
Block2	462 (74%)	0 (0%)	12,762 (2%)	53,886 (23%)	18 (18%)
Block3	584 (93%)	0 (0%)	20,839 (4%)	88,055 (38%)	84 (87%)

feature map arrays of the larger model that has three ODEBlocks (Block3) can be implemented on BRAM and URAM of the FPGA without using external DRAMs. In addition, parallelization of multiply-add operations is very common, but in this case, the original parameter and feature map arrays are further partitioned based on the degree of parallelism. Unfortunately, these array partitionings increase BRAM and URAM utilizations due to underutilized BRAM and URAM instances since their instance sizes are 36kb and 288kb, respectively. Although our Block2 implementation could be parallelized, our Block3 case could not be parallelized due to the slightly increased URAM utilization. As

a result, Table 5 shows the results without parallelization in order to show their minimum resource utilization (thus, their resource utilization will be increased depending on the degree of parallelism).

Regarding the performance, Table 6 shows the execution time of each block in the cases of FPGA (PL and PS) and CPU (PS only). ‘‘Conv’’ indicates a total execution time of convolutional layers of a block by PL part of the FPGA.

Table 6: Execution time of each block on FPGA

	FPGA (PL and PS)		CPU (PS only)	Speedup
	Conv (ms)	Total (ms)	Total (ms)	
ODEBlock1	0.449	13.80	445	32.2
Downsampling1	7.512	7.75	384	49.5
ODEBlock2	0.597	14.40	400	27.8
Downsampling2	1.616	2.72	54	19.9
ODEBlock3	0.997	21.20	397	18.7
DMA transfer	0.329	0.35	0	-
Total		60.23	1681	27.9

This is a latency for processing a single sample for prediction. In the case of FPGA (PL and PS), a DMA transfer time between PS and PL parts (both directions) is additionally needed. In total, FPGA (PL and PS) is faster than CPU (PS only) by 27.9 times. Please note that, although a single execution time of Downsampling1 is quite large compared to ODEBlocks, ODEBlocks are repeatedly executed  $C$  times and their impact is higher than those of Downsampling1 and Downsampling2. Also, a further performance improvement of the FPGA can be expected by the parallelization of multiply-add operations, which was not done in this work due to the URAM utilization.

## 5 Summary

In this paper, a combination of Neural ODE and Depthwise Separable Convolution, called dsODENet, is designed and implemented for FPGAs. dsODENet is applied to a distillation-based edge domain adaptation as a student model. All the dsODENet blocks except the pre- and post-processing layers are implemented on PL part of Xilinx Zynq UltraScale+ FPGA and the others are executed on PS part. All their parameter and feature map arrays are stored in URAM and BRAM modules of the FPGA without relying on external DRAMs. It is evaluated in terms of domain adaptation accuracy, training speed, FPGA resource utilization, and speedup rate compared to a software execution. Regarding the domain adaptation accuracy, a student model of dsODENet is comparable to or better than that of ODENet and also better than some existing domain adaptation methods. The total parameter size of dsODENets without pre- and post-processing layers is reduced by 54.2% to 79.8%. The FPGA implementation accelerates the prediction tasks by 27.9 times faster than a software implementation on PS part.

As a future work, although BRAM and URAM utilizations are currently quite high to further partition them, we are working on parallelization of multiply-add operations of the convolutional layers by introducing 16-bit fixed-point or bfloat16 representations to suppress the on-chip memory utilizations and enable the further partitioning for the parallel implementation.

## References

- [1] Franois Chollet. Xception: Deep Learning with Depthwise Separable Convolutions. In *Proceedings of the IEEE Conference on Computer Vision and Pattern Recognition (CVPR)*, pages 1800–1807, Jul 2017.
- [2] Andrew G. Howard, Menglong Zhu, Bo Chen, Dmitry Kalenichenko, Weijun Wang, Tobias Weyand, Marco Andreetto, and Hartwig Adam. MobileNets: Efficient Convolutional Neural Networks for Mobile Vision Applications. arXiv:1704.04861, 2017.
- [3] Kaiming He, Xiangyu Zhang, Shaoqing Ren, and Jian Sun. Deep Residual Learning for Image Recognition. arXiv:1512.03385, 2015.
- [4] Ricky T. Q. Chen, Yulia Rubanova, Jesse Bettencourt, and David Duvenaud. Neural Ordinary Differential Equations. In *Proceedings of the Annual Conference on Neural Information Processing Systems (NeuroIPS’18)*, pages 6572–6583, Dec 2018.
- [5] Hirohisa Watanabe and Hiroki Matsutani. Accelerating ODE-Based Neural Networks on Low-Cost FPGAs. In *Proceedings of the IEEE International Parallel and Distributed Processing Symposium (IPDPS’21) Workshops*, pages 88–95, Mar 2021.

- [6] Jianfei Yang, Han Zou, Shuxin Cao, Zhenghua Chen, and Lihua Xie. MobileDA: Toward Edge-Domain Adaptation. *IEEE Internet of Things Journal*, 7(8):6909–6918, Aug 2020.
- [7] Baochen Sun and Kate Saenko. Deep CORAL: Correlation Alignment for Deep Domain Adaptation. arXiv:1607.01719, 2016.
- [8] Kate Saenko, Brian Kulis, Mario Fritz, and Trevor Darrell. Adapting Visual Category Models to New Domains. *Proceedings of the European Conference in Computer Vision (ECCV’10)*, 6314:213–226, Sep 2010.
- [9] Yaroslav Ganin and Victor Lempitsky. Unsupervised Domain Adaptation by Backpropagation. In *Proceedings of the International Conference on Machine Learning (ICML’15)*, pages 1180–1189, Jul 2015.
- [10] Johannes Stalkamp, Marc Schlipf, Jan Salmen, and Christian Igel. The German Traffic Sign Recognition Benchmark: A Multi-class Classification Competition. In *Proceedings of the International Joint Conference on Neural Networks (IJCNN’11)*, pages 1453–1460, Aug 2011.
- [11] Yuval Netzer, Tao Wang, Adam Coates, Alessandro Bissacco, Bo Wu, and Andrew Ng. Reading Digits in Natural Images with Unsupervised Feature Learning. In *Proceedings of the NIPS Workshop on Deep Learning and Unsupervised Feature Learning*, Dec 2011.
- [12] Y. Lecun, L. Bottou, Y. Bengio, and P. Haffner. Gradient-based Learning Applied to Document Recognition. *Proceedings of the IEEE*, 86(11):2278–2324, 1998.
- [13] Mingsheng Long, Zhangjie Cao, Jianmin Wang, and Michael I Jordan. Conditional Adversarial Domain Adaptation. In *Proceedings of the Annual Conference on Neural Information Processing Systems (NeuroIPS’18)*, pages 1640–1650, Dec 2018.
- [14] Konstantinos Bousmalis, George Trigeorgis, Nathan Silberman, Dilip Krishnan, and Dumitru Erhan. Domain Separation Networks. In *Proceedings of the Annual Conference on Neural Information Processing Systems (NeuroIPS’16)*, pages 343–351, Dec 2016.
- [15] Eric Tzeng, Judy Hoffman, Kate Saenko, and Trevor Darrell. Adversarial Discriminative Domain Adaptation. In *Proceedings of the IEEE Conference on Computer Vision and Pattern Recognition (CVPR’17)*, pages 2962–2971, Jul 2017.